Non-destructive characterisation of mesenchymal stem cell differentiation using LC-MS-based metabolite footprinting

Amal Surrati [1], Rob Linforth [2], Ian D. Fisk [2], Virginie Sottile [1]*, Dong-Hyun Kim [3]*.

[1]Wolfson Centre for Stem Cells, Tissue, Engineering and Modelling (STEM), School of Medicine, The University of Nottingham, CBS Building - University Park, Nottingham NG7 2RD (U.K.)

[2]Division of Food Sciences, University of Nottingham, Sutton Bonington Campus, Sutton Bonington, Leicestershire, LE12 5RD (U.K.)

[3]Centre for Analytical Bioscience, Division of Molecular and Cellular Sciences, School of Pharmacy, The University of Nottingham, Nottingham, NG7 2RD (U.K.)

*Correspondence to: Email: virginie.sottile@nottingham.ac.uk Tel: +44 1158231235
Email: dong-hyun.kim@nottingham.ac.uk Tel: +44 1157484697

Abstract

Bone regeneration is a complex biological process where major cellular changes take place to support the osteogenic differentiation of mesenchymal bone progenitors. To characterise these biological changes and better understand the pathways regulating the formation of mature bone cells, the metabolic profile of mesenchymal stem cell (MSC) differentiation *in vitro* has been assessed non-invasively during osteogenic (OS) treatment using a footprinting technique. Liquid chromatography (LC)-mass spectrometry (MS)-based metabolite profiling of the culture medium was carried out in parallel to mineral deposition and alkaline phosphatase activity which are two hallmarks of osteogenesis *in vitro*. Metabolic profiles of spent culture media with a combination of univariate and multivariate analyses investigated concentration changes of extracellular metabolites and nutrients linked to the presence of MSCs in culture media. This non-invasive LC-MS-based analytical approach revealed significant metabolomic changes between the media from control and OS-treated cells showing distinct effects of MSC differentiation on the environmental footprint of the cells in different conditions (control vs OS treatment). A subset of compounds was directly linked to the osteogenic time-course of differentiation, and represent interesting metabolite candidates as non-invasive biomarkers for characterising the differentiation of MSCs in a culture medium.

Keywords: LC-MS, Metabolite footprinting, Mesenchymal stem cell, Osteogenesis, Non-destructive stem cell phenotyping, Stem cell differentiation

Introduction

During skeletal development or fracture repair, bone is formed by a complex process involving the osteogenic differentiation of mesenchymal progenitors [1]. This process requires a variety of intracellular and extracellular molecular mechanisms orchestrating specialised cell types [1, 2]. Mesenchymal stem cells (MSCs) are multipotent somatic progenitors able to differentiate into osteogenic, chondrogenic and adipogenic lineages [3]. Their capacities to generate new osteoblasts, the bone-forming cell type, and the possibility of harvesting them from bone marrow collections have made them a promising candidate for therapeutic approaches to skeletal repair [4]. Numerous *in vitro* studies have demonstrated the effect of osteoinductive treatment combining dexamethasone, ascorbic acid, and beta-glycerophosphate (βGP) on MSC osteogenesis. Dexamethasone induces osteogenesis *in vitro* through activating WNT/β-catenin signalling-dependent *Runx2* expression [5], whereas ascorbic acid increases collagen type 1 secretion [6, 7]. βGP provides inorganic phosphate (Pi) that facilitates intracellular signalling molecules [8, 9, 10].

Since metabolites provide the phenotypic outcome of gene expression or metabolic activities of a cell, global metabolite profiling can give a rapid snapshot of the cell physiology by monitoring concentration changes of a broad range of metabolites and provide insight into relationships between genotype and phenotype [11, 12]. Therefore, metabolomics has been used widely for understanding underlying molecular processes in applications for human health and disease including biomarker and drug discovery [13]. Recent studies have reported changes in specific metabolites extracted from mesenchymal cultures in response to different microenvironment properties [14]. Furthermore, parathyroid hormone (PTH) effect on mouse osteogenic lineage was shown to be negatively influenced by suppressing cellular oxidation of glucose through tricarboxylic acid cycle (TCA cycle) [15]. Also, stimulation of glutamine biosynthesis through WNT signalling boosts osteoblasts formation [16]. In addition, studying mesenchymal stem cells in terms of osteogenic metabolomics would not only extend the understanding of bone tissue biology but also provide new approaches for pharmacological and clinical developments.

Metabolite profiling of intracellular metabolites is informative to understanding complex biological processes and systems, but this approach requires complicated sample preparation, including the rapid quenching of metabolism and extraction of intracellular metabolites from cells. Incomplete quenching and extraction methods could lead to biased quantification, due

to rapid turnover and loss of metabolites. Therefore, an alternative approach can be the measurement of extracellular metabolites that are secreted and/or excreted from cells into their growth media or nutrients that are consumed by cells. This metabolite footprinting technique requires minimum sample preparation and can provide significant information to understand the microenvironment of a cell of interest [17, 18], as used for human hepatic stem cells (hHpSCs) [19].

Liquid chromatography (LC)-mass spectrometry (MS) is a powerful tool for the quantification of small molecules, as well as the identification of known and unknown metabolites in biological samples. Recently, LC-MS-based approaches have been employed widely for the quantitative analysis of extracellular metabolites and nutrients in a growth medium [20], it is therefore reasonable to speculate that MSC differentiation could be characterised by its distinct metabolic footprint, including metabolite secretion and/or excretion and nutrient consumption, which may be unique to the specific metabolic pathways activated during MSC differentiation. The pathways identified by LC-MS-based footprinting were proposed to be used to monitor stem cell differentiation through the analysis of metabolite changes not only between various cell fates, but also at different stages within specific lineage maturation.

Established cell phenotyping methods including gene expression analysis, protein immunodetection and flow cytometry are widely used to produce high resolution molecular phenotyping at the cellular and population level [21, 22, 23], however these approaches involve invasive and cell destructive steps which limit their application to live cell monitoring. This study proposes a non-invasive analysis approach for metabolic changes occurring in the culture medium during MSC osteogenic differentiation, and for the first time, demonstrates a quantitative time-point analysis of key molecular changes occurring during MSC osteogenesis.

Material and methods

Materials were purchased from Life Technologies (Paisley, UK) unless otherwise stated.

Cell culture and differentiation assay

Mouse mesenchymal stem cells (MSCs) [24] were seeded in 22.5mm x 75.5mm vials (Fisher Scientific, UK) as six replicates at density of $3x10^4$ cells/mL in standard MSC medium

consisting of Dulbecco's Modified Eagle's Medium (DMEM), 10 % fetal calf serum (FCS), 1 mM L-glutamine, 1 % non-essential amino acids and 10 % antibiotics, and incubated at 37 °C in 5 % CO_2. Confluent cells treated with osteogenic medium consisting of standard MSC medium, 100 nm dexamethazone (Sigma-Aldrich, Gillingham, UK), 0.05 mM L-ascorbic acid 2 phosphate (Acros Organics, Geel, Belgium) and 10 mM beta glycerophosphate (βGP, Sigma-Aldrich), and treated for 15 days with medium changes every 2 days. Cell maintained in standard MSC medium were used as a control medium sample. All supplements were prepared according to the manufacturer's guidelines. The same media, reagents and supplements were used throughout the experiment for consistency.

Calcium deposits were analysed using Alizarin Red staining. At the stated time point, cells from 4 replicates were trypsinised and pellets were smeared onto glass slides, air dried, fixed with 100 % methanol and washed with distilled water. Slides were incubated in 1 % Alizarin Red staining solution (Sigma-Aldrich) for 10 min at room temperature, and washed with distilled water until all excess stain had been removed. Mineral deposits were then observed using a Nikon Eclipse Ni90 light microscope. In parallel, Alkaline phosphatase (ALP) activity was measured in the remaining two culture replicates using 100 µL SIGMA FAST p-Nitrophenyl Phosphate reagent (Sigma-Aldrich) for 20 min at 37 °C, 5% CO_2. 100 µL from each sample transferred to a 96 well plate were analysed in triplicate using an Tecan Infinite 200 plate reader and Tecan-i-control 1.10 software to measure absorbance at 405 nm. Quantification of ALP absorbance was not normalized to the cell number present in each vial.

Metabolites extraction

At day 5, 10 and 15, 1 mL of the medium in each culture (MSC-conditioned medium) was collected and centrifuged at 7378 g for 5 min. 250 µL of the collected medium were transferred to a new tube for extraction and protein precipitation by adding 750 µL of cold methanol in a ratio of 1:4, then mixing vigorously and incubating at -20 °C for 20 min. After incubation, samples were centrifuged at 13,200 g at 4 °C for 10 min, transferred to pre-cooled tubes and stored at -80 °C until LC-MS analysis. Samples of fresh standard MSC medium and OS medium were processed in parallel as no cells controls. All samples were prepared as six biological replicates, and the experiment was run as two successive independent repeats. An equal mix of all samples was prepared as quality control (QC) for instrument performance assessment [25].

Analytical methodologies

For metabolite footprinting of spent culture media, LC-MS was performed on an Accela system coupled to an Exactive MS (Thermo Fisher Scientific, Hemel Hempstead, UK). Spectral data was acquired in full scan ion mode (m/z 70-1,400, resolution 50,000) in both positive and negative electrospray ionisation modes. The probe temperature and capillary temperature were maintained at 150 and 275 °C, respectively. The calibration mass range was extended to cover small metabolites by inclusion of low-mass contaminants with the standard Thermo calibration mixture masses (below m/z 1400), $C_2H_6NO_2$ for positive ion electrospray ionisation (PIESI) mode (m/z 76.0393) and $C_3H_5O_3$ for negative ion electrospray ionisation (NIESI) mode (m/z 89.0244). Chromatographic separation was carried out using a ZIC-pHILIC (150 mm × 4.6 mm, 5 µm column, Merck Sequant) maintained at 45 °C and a flow rate of 300 µL/min as previously described in [26]. Briefly, the mobile phase consisted of (A) 20 mM ammonium carbonate in water, (B) 100 % acetonitrile which were eluted with a linear gradient from 80 % B to 5 % B over 15 min, followed by a 2 min linear gradient from 5 % B to 80 % B, and 7 min re-equilibration with 80% B. The injection volume was 10 µL and samples were maintained at 4 °C.

Metabolites identification process

LC-MS raw data from medium samples (control medium samples and their blanks, OS treated medium samples and their blanks and QC samples and reagent blanks) were processed with XCMS for untargeted peak-picking [27], and peak matching and annotation of related peaks were carried out using mzMatch [28]. IDEOM with the default parameters was used for noise filtering and putative metabolite identification. Level 1 metabolite identification was performed by matching accurate masses and retention times of authentic standards which were run on the same instrument according to the metabolomics standards initiative [29, 30], but Level 2 putative identification was considered when standards were not available and predicted retention times were employed.

Supervised orthogonal partial least squares discriminant analysis (OPLS-DA) [31] was initially performed by SIMCA-P 13.0.2 version (Umetrics AB, Umea, Sweden) (i) for general visualisation of metabolite differences between control medium samples and their controls, and OS treated medium samples and their blanks, (ii) to identify the temporal shift within control and OS treated conditions, and (iii) to observe the differences between control and OS treated medium samples (n=6 in each group). Mass ions for discriminant biomarkers were

selected by variable importance in projection values (VIP) where VIP values greater than one were considered as potential biomarkers. In addition to the investigation of VIP scores from OPLS-DA for the discovery of key discriminatory metabolites, univariate anlaysis was applied as a final feature selection. One-way ANOVA was carried out using Metaboanalyst that is a web server for metabolomic data analysis and interpretation [32], and was used to evaluate levels of significant difference between control and OS treated media.

Result and Discussion

In vitro model of osteogenic differentiation

In order to model the cellular changes occurring upon osteogenic induction, mesenchymal stem cells (MSC) were treated *in vitro* to induce osteogenic differentiation (Fig. 1), and the cultures were analysed at day 5, 10 and 15 to investigate changes in alkaline phosphatase activity (ALP) and mineral content, which are two major characteristics of bone formation [33]. No mineralisation was detected with standard medium, whilst OS conditions showed mineral deposits that were positively stained at day 10 and strongly at day 15 (Fig. 1A). ALP levels increased at early stages of OS induction with significant elevation toward day 10, followed by a notable decline toward day 15, when ALP activity returned to comparable levels to standard control medium (Fig. 1B), in line with previous reports [34]. The ALP changes and associated mineral deposits accumulation during osteogenic treatment containing ascorbic acid and beta glycerophosphate confirmed MSC differentiation during the 15-day time course [35, 36].

Multivariate analysis of LC-MS profiling data

In order to investigate the changes occurring in the MSC culture medium over the 15-day treatment period (Supplementary Fig.1), samples from standard medium cultures, OS-treated cultures, and their respective blank media (not exposed to cells) were analysed by LC-MS. LC-MS data from these MSC-conditioned or blank media samples were transformed into 2D matrix by mzMatch, to introduce an exact mass and retention time for each mass ion. OPLS-DA was then performed to determine the overall biological variation between all conditions, and to identify noticeable trends upon conditioning with MSCs, and over the course of the OS treatment.

OPLS-DA scores plots showed reproducible clustering of six biological replicates for each sample group, and highlighted clear differences between the different conditions tested (Fig. 2). The non-conditioned fresh media (blanks) analysed in the absence of MSCs showed distinct clusters from each spent culture medium conditioned in the presence of MSCs (control and OS medium samples) with R2 and Q2 values of 0.841 and 0.644, respectively (Fig. 2A). Similarly, samples exposed to osteogenic medium clustered in a different quadrant from the standard control medium samples in the OPLS-DA scores plot. This multivariate analysis clearly showed that LC-MS-based metabolite footprinting was able to non-invasively detect changes of metabolites according to cell differentiation. From separate scores plots of either standard control or OS medium conditioned (Fig. 2B-C), the scores of all cell-conditioned samples (at day 5, 10 and 15) showed a significant shift away from their respective fresh media (blanks), indicating a distinctive MSC-related metabolomic signature. The OPLS-DA models were cross-validated by calculating Q2 which is an estimate of the predictive ability of the model. The obtained R2 and Q2 values from OPLS-DA models of each sample were 0.991 and 0.756 for standard control medium, and 0.992 and 0.777 for OS medium conditioned, respectively, demonstrating an acceptable model. As clearly shown in Fig. 2B and C, the scores of fresh media in the absence of cells are observed in the middle left hand side, and as the length of culture under treatment increased, the cluster spread from left to right (D5 and 10) and then goes to the bottom (D15). These resultant scores plots clearly showed cluster patterns directly related to the length of cell culture treatment. It is therefore reasonable to consider that the metabolite footprinting data from MSC cell culture media analysed using LC-MS contains valuable information regarding metabolite secretion/excretion and nutrient consumption relevant to the metabolic effect of MSC differentiation.

Changes in MSC medium were monitored over the 15-day differentiation time-course. When comparing the three time-points analysed within each treatment group, distinct differences were observed suggesting dynamic changes in the MSC culture medium over time following the same trend in both standard and OS treatment conditions, with datasets at early culture stages (day 5 and 10) showing closer metabolomic proximity than the late time-point (day 15).

Feature selection: Analysis of MSC culture samples versus blank media without cells

To determine which mass ions contributed to the clusters and trends between MSC cultured media and medium only blank samples, group comparisons were performed between fresh medium (day 0) and day 15 samples within the OPLS-DA models. Key mass ions for discriminant biomarkers were selected by VIP values higher than one were considered as potential key mass ions. In addition to the multivariate analysis, univariate one-way ANOVA testing was also performed to identify significant compounds consumed and excreted by MSCs (both in standard and OS treatments) compared to their medium-only blanks over time. Key mass ions were also selected from the univariate analysis with the false discovery rate Q ≤ 0.05. The analysis was repeated in two independent experiments, and the combination of multi- and univariate analyses identified 215 metabolites showing variation between the MSC-conditioned medium samples compared to matching medium-only blanks, both under control medium and OS treatment (Supplementary table 1). A pie chart showing the classification of 195 metabolites according to their metabolism was generated by focusing on compounds selectively increased in the presence of MSCs (Fig. 3), and a heatmap showing their fold changes is presented in Supplementary Fig. 2.

This first analysis identified significant metabolomic changes related to MSC conditioning of the culture medium, such as the increase of deoxyuridine, orotidine, indole-3-acetaldehyde, acronycidine, (S)-3-methyl-2-oxopentanoic acid, 1-methylnicotinamide, 2-hydroxy-4-methylthiobunoate, 3-(4-hydroxyphenyl)pyruvate (Fig.4). Some of these compounds are linked to cell proliferation. For instance, deoxyuridine is involved in the synthesis of nucleosides, the structural subunits of nucleic acids [37], and are known to fluctuate during DNA synthesis or the S-phase of the cell cycle [38, 39]. Similarly, orotidine is involved in nucleotide synthesis through pyrimidine synthesis (KEGG pathway; MAP00240). In our study, LC-MS-based footprinting detected changes in deoxyuridine and orotidine in culture medium conditioned by MSCs. During OS treatment, deoxyuridine significantly increased while orotidine decreased compared to MSC conditioned medium under control conditions. This finding could suggest epimetabolomic changes during nucleotide synthesis over the osteogenic differentiation time-course.

In addition, L-tryptophan, which is an essential amino acid for protein synthesis [40] and one of the essential component of DMEM, was found at comparable levels in all medium conditions including medium only blanks (data not shown). Indole-3-acetaldehyde, a derivative of L-tryptophan reported during gluconeogenesis [41, 42], was significantly increased in medium conditioned by MSCs, suggesting that indol-3-acetaldehyde might have been formed from the

L-tryptophan present in the culture medium (DMEM). Our data also showed a significant elevation in 1-methylnicotinamide upon MSC culture and during osteogenesis compared to the control medium conditions. 1-methylnicotinamide is reported as a nicotinamide metabolite [43], and a reduction in nicotinamide adenine dinucleotide (NADH) intensity has previously been observed in MSCs following osteogenic differentiation [44], suggesting that metabolomic changes in NADH metabolism may reflect different stages of osteogenic maturation.

Non-invasive metabolic profiling of MSC osteogenic differentiation

Further investigation was carried out to identify metabolomic differences between MSC-conditioned medium produced under standard and OS treatment. Out of 195 compounds initially detected as potential biomarkers, 21 metabolites increased specifically during OS differentiation of MSCs (Table 1).

Measurements of these compounds over the culture time-course showed significant upregulation of citrate, cis-aconitate, 2-oxoglutarate (α-ketoglutarate derivative), succinate, glycerol and orthophosphate in MSC medium upon OS exposure (Fig. 5). Conversely, the concentration of sn-glycerol-3-phosphate was rapidly diminished from the OS-treated medium over time. Interestingly, compounds such as sn-glycerol 3-phosphate, glycerol, orthophosphate, glutamate and citrate are linked to the degradation of βGP added to OS medium, which is hydrolysed by the glycerol 3-phosphatase enzyme to glycerol and orthophosphate during glycerolipid metabolism (KEGG REACTION: R00841) (KEGG ENZYME: EC3.1.3.19). Higher levels of glycerol and orthophosphate were consistently detected throughout osteogenic differentiation time-course (Fig. 5F-G). Although orthophosphate was increased with osteogenic treatment, the LC-MS technique detected low concentration of this compound in the standard medium control, possibly due to other metabolic processes such as glutamine metabolism by L-glutamine synthetase enzyme (ATP + L-glutamate + ammonia <=> ADP + orthophosphate + L-glutamine) (KEGG REACTION: R00253) and the Citrate cycle (ATP + citrate + CoA <=> ADP + orthophosphate + acetyl-CoA + oxaloacetate) (KEGG ENZYME: 2.3.3.8). Furthermore, orthophosphate could play a role in ALP inhibition at late stages of osteogenic differentiation by binding to the enzyme active site and inhibiting its activity [45]. This could indicate a link between the noticeable orthophosphate elevation toward day 15 of differentiation and the reduction in ALP level in day 15 OS-treated cells (Fig.1B).

A subset of compounds differentially detected in OS culture medium could also be related to the Krebs cycle (Fig. 6). Citrate, cis-aconitate, α-ketoglutarate, succinate, malonate and malate are component of the Krebs cycle or Tricarboxylic cycle (TCA cycle), which represents an essential energy metabolism pathway in cells as first described by H.A. Krebs [46]. In the typical Krebs cycle, pyruvate produced by glycolysis is converted to acetyl-CoA by the pyruvate dehydrogenase complex. Acetyl-CoA then enters the mitochondria and combines to oxaloacetate to produce citrate (through the citrase synthesase enzyme) which is then utilised to form cis-aconitate. The later becomes isocitrate, is then oxidised to form oxoglutarate (α-ketoglutarate derivative), followed by conversion of succinyl-CoA to succinate with GTP production. Succinate will then converts to fumarate and malate, completing the cycle to form oxaloacetate. Significant changes in levels of Krebs cycle metabolites were identified in the medium of MSC cultures under both standard and osteogenic conditions. LC-MS analysis indicated a substantial and gradual increase in citrate and cis-aconitate production throughout osteogenic induction (peaking at day 15) in comparison with standard medium control. Interestingly, citric acid has been described as essential for bone organic nanostructure [47] and bone tissue engineering in bone marrow-derived rat MSCs [48]. This suggests that the change in citrate levels may be linked to osteogenic treatment. Cis-aconitate is an intermediate step in cell respiration, however there is no report to date describing the possible effect of this compound on osteogenesis.

It was reported that 2-oxoglutarate (α-ketoglutarate derivative) is a precursor of hydroxyproline, which is essential amino acid for bone protection [49]. Interestingly, in our data 2-oxoglutarate shows a significant increase during osteogenic treatment compared to untreated control which could support its importance in bone protection.

Conclusion

In this study, extracellular metabolites were sampled and analysed at different time points during MSC osteogenic induction *in vitro*, leading to the identification of differentially regulated compounds linked to cellular changes in culture.

The therapeutic potential of mesenchymal stem cells for applications in regenerative medicine and drug discovery has warranted a number of investigations targeting conditions

such as osteoporosis and other conditions where skeletal tissue is compromised. Studies on osteogenic induction require the development of in-line, non-destructive characterisation methodologies to be able to phenotype MSCs during differentiation and limit the requirement for sacrificial cultures needed for most cellular and molecular techniques. In our study, for the first time, LC-MS-based footprinting with multi- and univariate analyses has been used for the non-destructive characterisation of MSC differentiation. OPLS-DA analysis from MSCs in undifferentiated and osteogenically-induced states showed significant and reproducible changes demonstrated by OPLS-DA scores plots from metabolic footprints of each condition. The MSC cultures samples analysed showed clear metabolomic changes during osteogenesis, with a particular prominence of compounds linked to cell respiration and the production of orthophosphate, which plays an important role in ALP level during bone differentiation. Further analysis of these metabolomic changes compared to cell proliferation dynamics will be useful to refine the profile of differentiation-related compounds.

Trends of individual OPLS-DA scores plots revealed MSC-related metabolic signatures, and were also able to clearly discriminate between medium samples from undifferentiated and OS treated cultures. Changes were followed during the 15-day differentiation kinetics and showed gradual shifts in the metabolomic profile of the culture medium. LC-MS spent culture medium analysis enabled the fine characterisation of stem cell environment, and showed it can generate a chemofootprint of differentiated cells amenable to real-time analysis of therapeutic cells in culture. These observations confirm the power of LC-MS to screen chemical compounds present in the cellular environment and quantitatively measure cell-based differences non-destructively. Combined to stable isotope assisted approaches [20, 50], this LC-MS technology could be used for future stem cell metabolite profiling to quantify intracellular metabolites involved in specific stages of differentiation and investigate specific pathways identified by the metabolite footprinting analysis in the current study.

Acknowledgments:

Some of the methods utilised were developed under the BBSRC Doctoral Training Partnership BB/F017014/1. The authors are grateful for the support of the Saudi Ministry of Higher Education (A.S.), and wish to thank Dr Kenneth Smith (School of Medicine, U. of Nottingham) for useful discussion.

REFERENCES

1. J. A. Buckwalter, M. J. Glimcher, R. R. Cooper and R. Recker, *Instr Course Lect*, 1996, **45**, 387-399.
2. J. A. Buckwalter, M. J. Glimcher, R. R. Cooper and R. Recker, *Instr Course Lect*, 1996, **45**, 371-386.
3. M. Dominici, K. Le Blanc, I. Mueller, I. Slaper-Cortenbach, F. Marini, D. Krause, R. Deans, A. Keating, D. Prockop and E. Horwitz, *Cytotherapy*, 2006, **8**, 315-317.
4. G. I. Im, *J Cell Biochem*, 2015, **116**, 487-493.
5. Z. Hamidouche, E. Hay, P. Vaudin, P. Charbord, R. Schule, P. J. Marie and O. Fromigue, *FASEB J*, 2008, **22**, 3813-3822.
6. R. T. Franceschi and B. S. Iyer, *J Bone Miner Res*, 1992, **7**, 235-246.
7. N. Jaiswal, S. E. Haynesworth, A. I. Caplan and S. P. Bruder, *J Cell Biochem*, 1997, **64**, 295-312.
8. B. L. Foster, F. H. Nociti, Jr., E. C. Swanson, D. Matsa-Dunn, J. E. Berry, C. J. Cupp, P. Zhang and M. J. Somerman, *Calcif Tissue Int*, 2006, **78**, 103-112.
9. S. Fatherazi, D. Matsa-Dunn, B. L. Foster, R. B. Rutherford, M. J. Somerman and R. B. Presland, *J Dent Res*, 2009, **88**, 39-44.
10. H. Tada, E. Nemoto, B. L. Foster, M. J. Somerman and H. Shimauchi, *Bone*, 2011, **48**, 1409-1416.
11. S. G. Oliver, M. K. Winson, D. B. Kell and F. Baganz, *Trends Biotechnol*, 1998, **16**, 373-378.
12. D. H. Kim, J. W. Allwood, R. E. Moore, E. Marsden-Edwards, W. B. Dunn, Y. Xu, L. Hampson, I. N. Hampson and R. Goodacre, *Mol Biosyst*, 2014, **10**, 398-411.
13. M. P. Quinones and R. Kaddurah-Daouk, *Neurobiol Dis*, 2009, **35**, 165-176.
14. P. Tsimbouri, N. Gadegaard, K. Burgess, K. White, P. Reynolds, P. Herzyk, R. Oreffo and M. J. Dalby, *J Cell Biochem*, 2014, **115**, 380-390.
15. E. Esen, S. Y. Lee, B. M. Wice and F. Long, *J Bone Miner Res*, 2015, DOI: 10.1002/jbmr.2556.
16. C. M. Karner, E. Esen, A. L. Okunade, B. W. Patterson and F. Long, *J Clin Invest*, 2015, **125**, 551-562.
17. D. B. Kell, M. Brown, H. M. Davey, W. B. Dunn, I. Spasic and S. G. Oliver, *Nat Rev Microbiol*, 2005, **3**, 557-565.
18. H. M. Elsheikha, M. Alkurashi, K. Kong and X. Q. Zhu, *BMC Res Notes*, 2014, **7**, 406.
19. W. S. Turner, C. Seagle, J. A. Galanko, O. Favorov, G. D. Prestwich, J. M. Macdonald and L. M. Reid, *Stem Cells*, 2008, **26**, 1547-1555.
20. D. H. Kim, F. Achcar, R. Breitling, K. E. Burgess and M. P. Barrett, *Metabolomics*, 2015, **11**, 1721-1732.
21. M. Junkin and S. Tay, *Lab Chip*, 2014, **14**, 1246-1260.
22. D. Ponnaiyan and V. Jegadeesan, *Eur J Dent*, 2014, **8**, 307-313.
23. Z. Chen, C. S. de Paiva, L. Luo, F. L. Kretzer, S. C. Pflugfelder and D. Q. Li, *Stem Cells*, 2004, **22**, 355-366.
24. D. R. Diduch, M. R. Coe, C. Joyner, M. E. Owen and G. Balian, *J Bone Joint Surg Am*, 1993, **75**, 92-105.
25. H. l. n. Pereira, J.-F. o. Martin, C. Joly, J.-L. Se´be´dio and E. Pujos-Guillot, *Metabolomics*, 2010, **6**, 207–218.
26. D. J. Creek, A. Jankevics, R. Breitling, D. G. Watson, M. P. Barrett and K. E. Burgess, *Anal Chem*, 2011, **83**, 8703-8710.

27. R. Tautenhahn, C. Bottcher and S. Neumann, *BMC Bioinformatics*, 2008, **9**, 504.
28. R. A. Scheltema, A. Jankevics, R. C. Jansen, M. A. Swertz and R. Breitling, *Anal Chem*, 2011, **83**, 2786-2793.
29. L. W. Sumner, A. Amberg, D. Barrett, M. H. Beale, R. Beger, C. A. Daykin, T. W. Fan, O. Fiehn, R. Goodacre, J. L. Griffin, T. Hankemeier, N. Hardy, J. Harnly, R. Higashi, J. Kopka, A. N. Lane, J. C. Lindon, P. Marriott, A. W. Nicholls, M. D. Reily, J. J. Thaden and M. R. Viant, *Metabolomics*, 2007, **3**, 211-221.
30. L. W. Sumner, Z. Lei, B. J. Nikolau, K. Saito and U. T. Roessner, R., *Metabolomics*, 2014, **10**, 1047.
31. J. Boccard and D. N. Rutledge, *Anal Chim Acta*, 2013, **769**, 30-39.
32. J. Xia, I. V. Sinelnikov, B. Han and D. S. Wishart, *Nucleic Acids Res*, 2015, **43**, W251-257.
33. R. S. Siffert, *J Exp Med*, 1951, **93**, 415-426.
34. G. S. Stein, J. B. Lian and T. A. Owen, *FASEB J*, 1990, **4**, 3111-3123.
35. L. D. Buttery, S. Bourne, J. D. Xynos, H. Wood, F. J. Hughes, S. P. Hughes, V. Episkopou and J. M. Polak, *Tissue Eng*, 2001, **7**, 89-99.
36. G. R. Beck, Jr., *J Cell Biochem*, 2003, **90**, 234-243.
37. S. Kit and Y. Minekawa, *Cancer Res*, 1972, **32**, 2277-2288.
38. C. L. Kaiser, A. J. Kamien, P. A. Shah, B. J. Chapman and D. A. Cotanche, *Laryngoscope*, 2009, **119**, 1770-1775.
39. C. Zeng, F. Pan, L. A. Jones, M. M. Lim, E. A. Griffin, Y. I. Sheline, M. A. Mintun, D. M. Holtzman and R. H. Mach, *Brain Res*, 2010, **1319**, 21-32.
40. E. R. Radwanski and R. L. Last, *Plant Cell*, 1995, **7**, 921-934.
41. J. Koga, K. Syono, T. Ichikawa and T. Adachi, *Biochim Biophys Acta*, 1994, **1209**, 241-247.
42. C. I. Pogson, D. M. Crisp and S. A. Smith, *Acta Vitaminol Enzymol*, 1975, **29**, 232-235.
43. K. Aoyama, K. Matsubara, K. Okada, S. Fukushima, K. Shimizu, S. Yamaguchi, T. Uezono, M. Satomi, N. Hayase, S. Ohta, H. Shiono and S. Kobayashi, *J Neural Transm (Vienna)*, 2000, **107**, 985-995.
44. H. W. Guo, C. T. Chen, Y. H. Wei, O. K. Lee, V. Gukassyan, F. J. Kao and H. W. Wang, *J Biomed Opt*, 2008, **13**, 050505.
45. E. E. Kim and H. W. Wyckoff, *J Mol Biol*, 1991, **218**, 449-464.
46. H. Kornberg and D. H. Williamson, *Biogr Mem Fellows R Soc*, 1984, **30**, 351-385.
47. Y. Y. Hu, A. Rawal and K. Schmidt-Rohr, *Proc Natl Acad Sci U S A*, 2010, **107**, 22425-22429.
48. A. Sanchez-Ferrero, A. Mata, M. A. Mateos-Timoneda, J. C. Rodriguez-Cabello, M. Alonso, J. Planell and E. Engel, *Biomaterials*, 2015, **68**, 42-53.
49. A. P. Harrison and S. G. Pierzynowski, *J Physiol Pharmacol*, 2008, **59 Suppl 1**, 91-106.
50. D. J. Creek, M. Mazet, F. Achcar, J. Anderson, D. H. Kim, R. Kamour, P. Morand, Y. Millerioux, M. Biran, E. J. Kerkhoven, A. Chokkathukalam, S. K. Weidt, K. E. Burgess, R. Breitling, D. G. Watson, F. Bringaud and M. P. Barrett, *PLoS Pathog*, 2015, **11**, e1004689.

FIGURE LEGENDS:

Figure 1: Osteogenic differentiation in MSC cultures after 5, 10 and 15 days. (A) Alizarin Red staining of cells treated with either control (top panel) or OS medium (bottom panel) showing no mineralization in control medium, while under OS treatment calcium deposits were identified at D10 and 15. (B) ALP activity assay showing an increase in response to OS treatment at day5 and 10. (*** $p<0.001$, ** $p<0.01$, * $p<0.05$; n=3). Scale bar= 200µm.

Figure 2: OPLS-DA scores plots of MSC medium samples from standard and OS-treatment, and their corresponding medium-only blanks, analysed after 5, 10 and 15 days in culture. (A) Combined standard and OS treated MSC-conditioned samples and their respective medium-only blanks (R2 = 0.841 and Q2= 0.644) (B) Untreated control medium MSC samples and their corresponding medium-only blanks (R2 = 0.991 and Q2= 756). (C) OS medium-treated MSC samples and their corresponding medium-only blanks (R2 = 992 and Q2= 777). Each condition was analysed in 6 biological replicates. Arrows indicate the metabolic profile changes between the sample conditions.

Figure 3: Functional categorisation of the nutrients and metabolites produced by MSCs in their culture medium. (A) 195 metabolites identified by LC-MS are categorised based on their biological function. (B) Venn diagram showing that within the total 195 identified metabolites, 10 were selectively increased in untreated control and 21 metabolites in OS treated medium.

Figure 4: MSC-related metabolites found to increase over time in culture medium in the presence of MSCs, both in control medium (blue triangle) and OS medium (red square), at day 5, 10 and 15 of culture. Zero peak intensity was defined by the level detected in medium only blanks. (**** $p<0.0001$, *** $p<0.001$** $p<0.01$, * $p<0.05$; n=6).

Figure 5: Metabolite changes identified in the culture medium MSC-related metabolites found to increase over time in culture medium in the presence of MSCs under OS treatment (red square) compared to control medium (blue triangle), at day 5, 10 and 15 of treatment. (**** $p<0.0001$, *** $p<0.001$** $p<0.01$, * $p<0.05$; n=6).

Figure 6: Biological pathways highlighted by the compounds differentially detected in MSC-conditioned culture medium (asterisk). (A) Components involved in cell respiration (Krebs

cycle) KEGG PATHWAY: MAP00020. (B) Components involved in βGP degradation to glycerol and orthophosphate.

Table 1: The most significant metabolites that were increased specifically during OS differentiation analysed by OPLS-DA and one-way ANOVA.

Exact mass	RT (min)	Formula	Putative metabolite	Identifier (PubChem)	↑ OS	ID confide
214.0244	9.68	$C_5H_{11}O_7P$	2-Deoxy-D-ribose 5-phosphate	CID:45934311	+	L2
112.0161	11.85	$C_5H_4O_3$	2-Furoate	CID:6919	++	L2
120.0059	11.54	$C_3H_4O_5$	2-Hydroxymalonate	CID:45	+	L2
192.0805	8.73	$C_{19}H_{28}O_6S$	3b-16a-Dihydroxyandrostenonesulfate	CID:22833522	+	L2
174.0164	11.70	$C_6H_6O_6$	cis-Aconitate	CID:643757	++	L2
192.027	11.88	$C_6H_8O_7$	Citrate	CID:311	++	L2
276.0958	10.99	$C_{10}H_{16}N_2O_7$	GammaGlutamylglutamicacid	CID:92865	++	L2
92.0474	8.77	$C_3H_8O_3$	Glycerol	CID:753	+	L1
246.0505	8.84	$C_6H_{15}O_8P$	Glycerophosphoglycerol	CID:439964	+	L2
262.0148	11.26	$C_9H_{10}O_7S$	Homovanillicacidsulfate	CID:29981063	+	L2
166.0477	9.49	$C_5H_{10}O_6$	L-Arabinonate	CID:5459849	+	L2
120.0423	7.90	$C_4H_8O_4$	L-Erythrulose	CID:5460032	+	L2
72.021	8.76	$C_3H_4O_2$	Methylglyoxal	CID:880	+	L1
146.0215	11.92	$C_5H_6O_5$	Methyloxaloacetate	CID:440890	+	L2
237.0849	11.88	$C_8H_{15}NO_7$	N-Acetyl-D-glucosaminate	CID:16126799	++	L2
217.1314	8.08	$C_{10}H_{19}NO_4$	O-Propanoylcarnitine	CID:107738	++	L2
97.9771	10.61	H_3O_4P	Orthophosphate	CID:1061	+	L2
102.0681	5.26	$C_5H_{10}O_2$	Pentanoate	CID:114781	++	L2
173.9986	4.89	$C_6H_6O_4S$	Unknown	CID:74426	+	L2
118.0267	10.09	$C_4H_6O_4$	Succinate	CID:1110	++	L1
139.978	12.05	$C_2H_4O_5S$	Sulfoacetate	CID:31257	+	L2

+ indicates the increase during OS treatment only compared to control medium samples, and ++ indicates an increase over time toward terminal differentiation (day 15).

ID Confidence: Metabolite identification level according to the metabolomics standards initiative (29,30); L1 – Level 1, L2 – Level 2

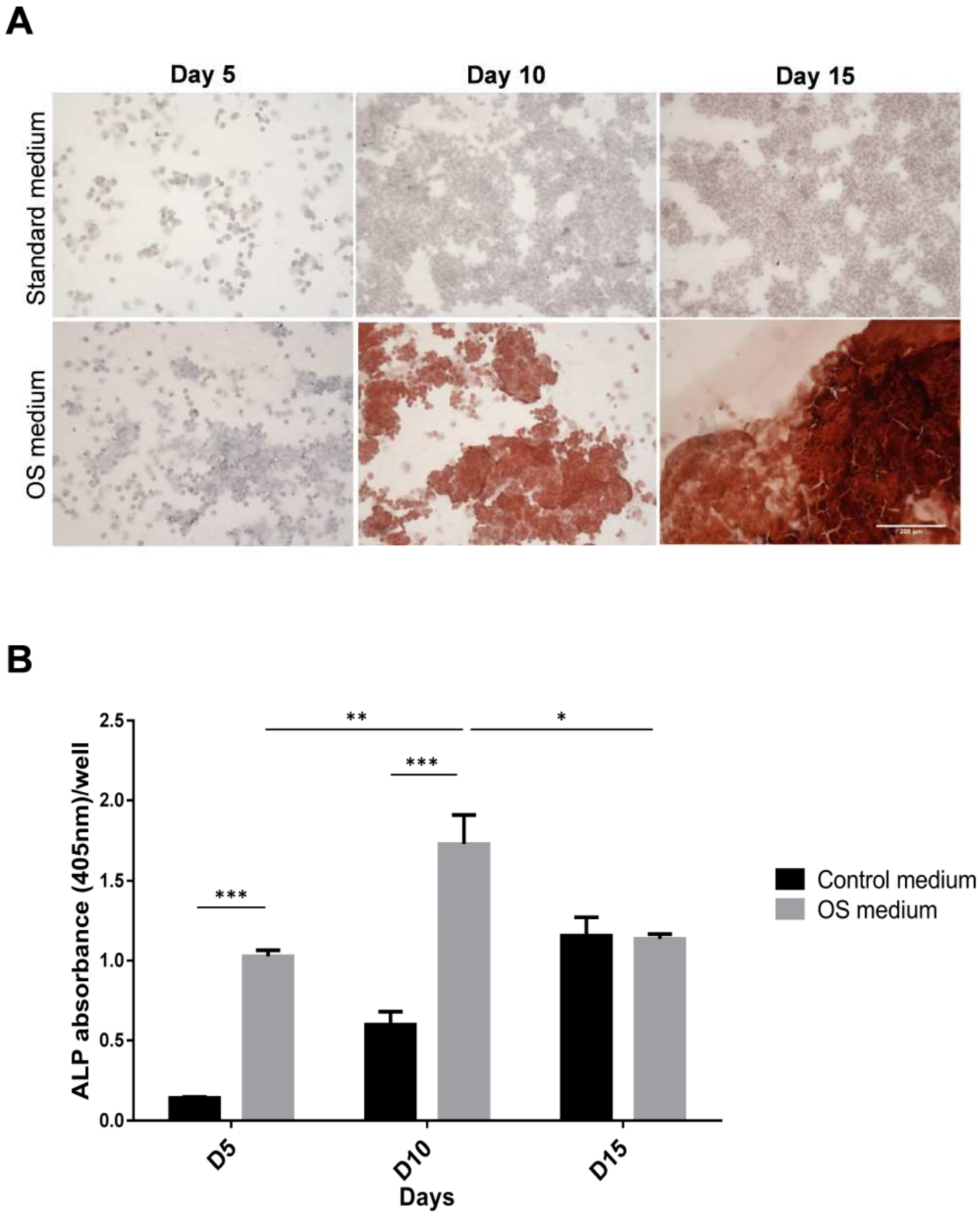
A
Day 5
Day 10
Day 15
Standard medium
OS medium
B
ALP absorbance (405nm)/well
2.5
2.0
1.5
1.0
0.5
0.0
**
*
***
***
D5
D10
D15
Days
Control medium
OS medium

Figure 1.

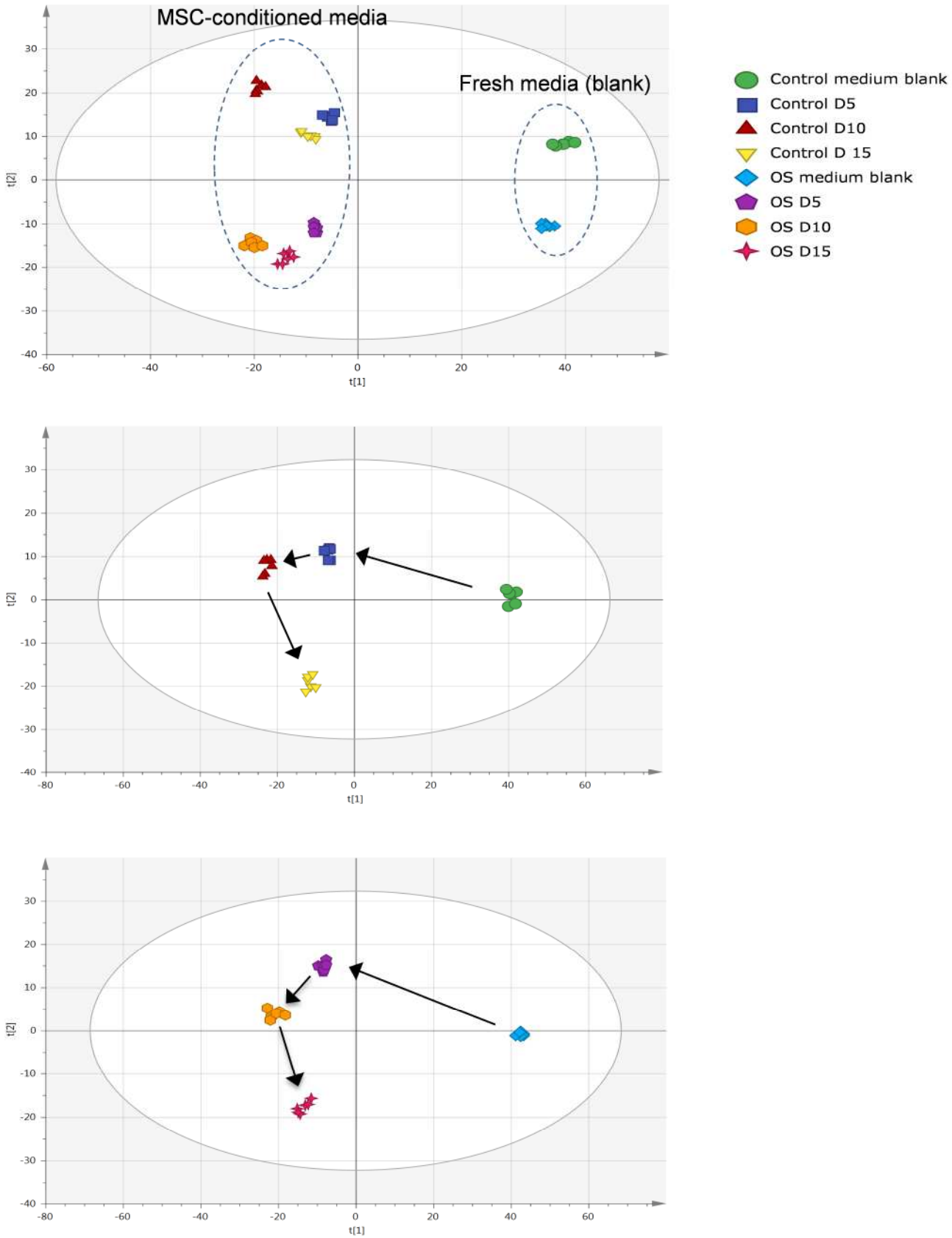
MSC-conditioned media
Fresh media (blank)
Control medium blank
Control D5
Control D10
Control D 15
OS medium blank
OS D5
OS D10
OS D15
t[1]
t[2]

Figure 2.

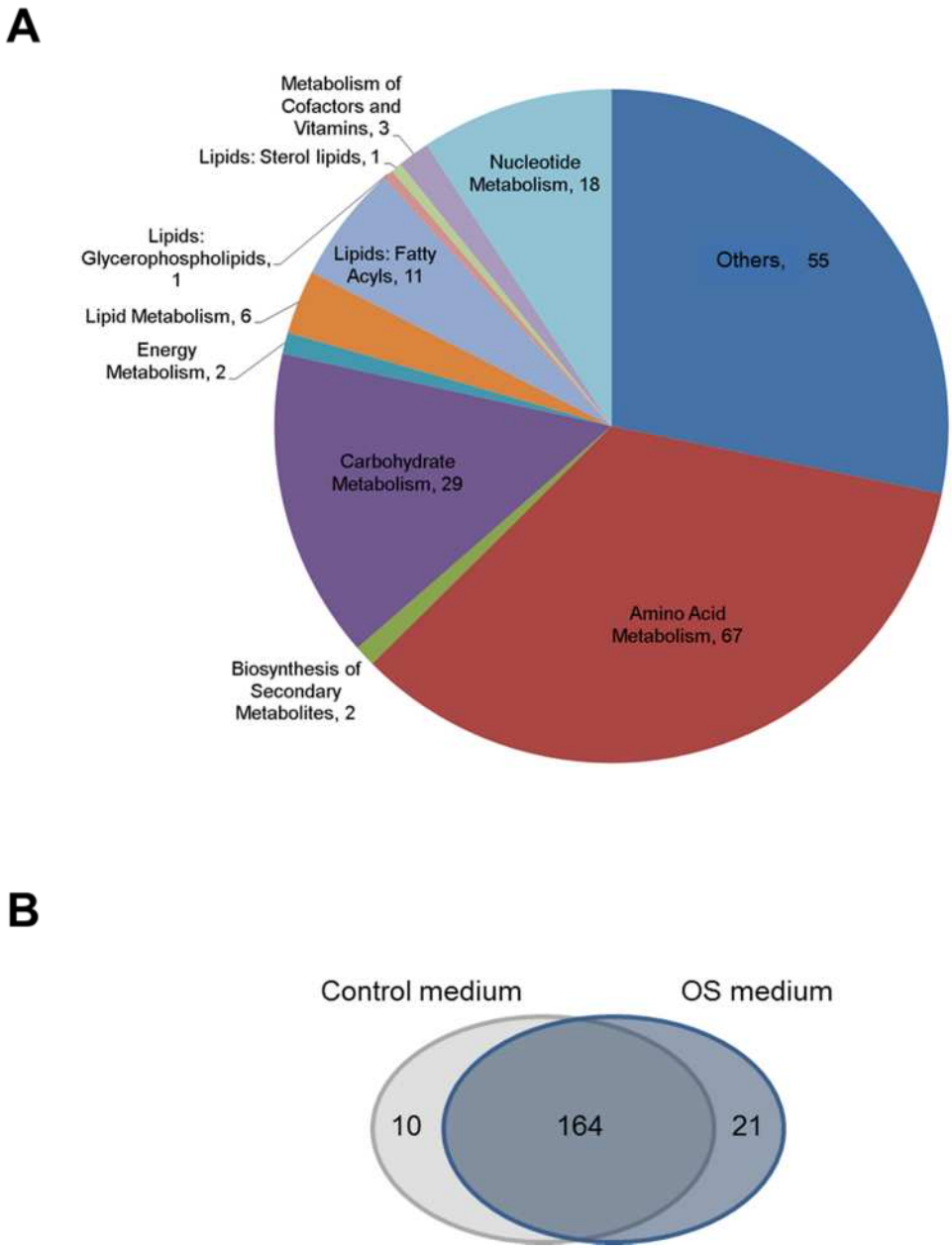
A
Metabolism of Cofactors and Vitamins, 3
Lipids: Sterol lipids, 1
Lipids: Glycerophospholipids, 1
Lipid Metabolism, 6
Energy Metabolism, 2
Nucleotide Metabolism, 18
Lipids: Fatty Acyls, 11
Others, 55
Carbohydrate Metabolism, 29
Amino Acid Metabolism, 67
Biosynthesis of Secondary Metabolites, 2
B
Control medium
OS medium
10
164
21

Figure 3.

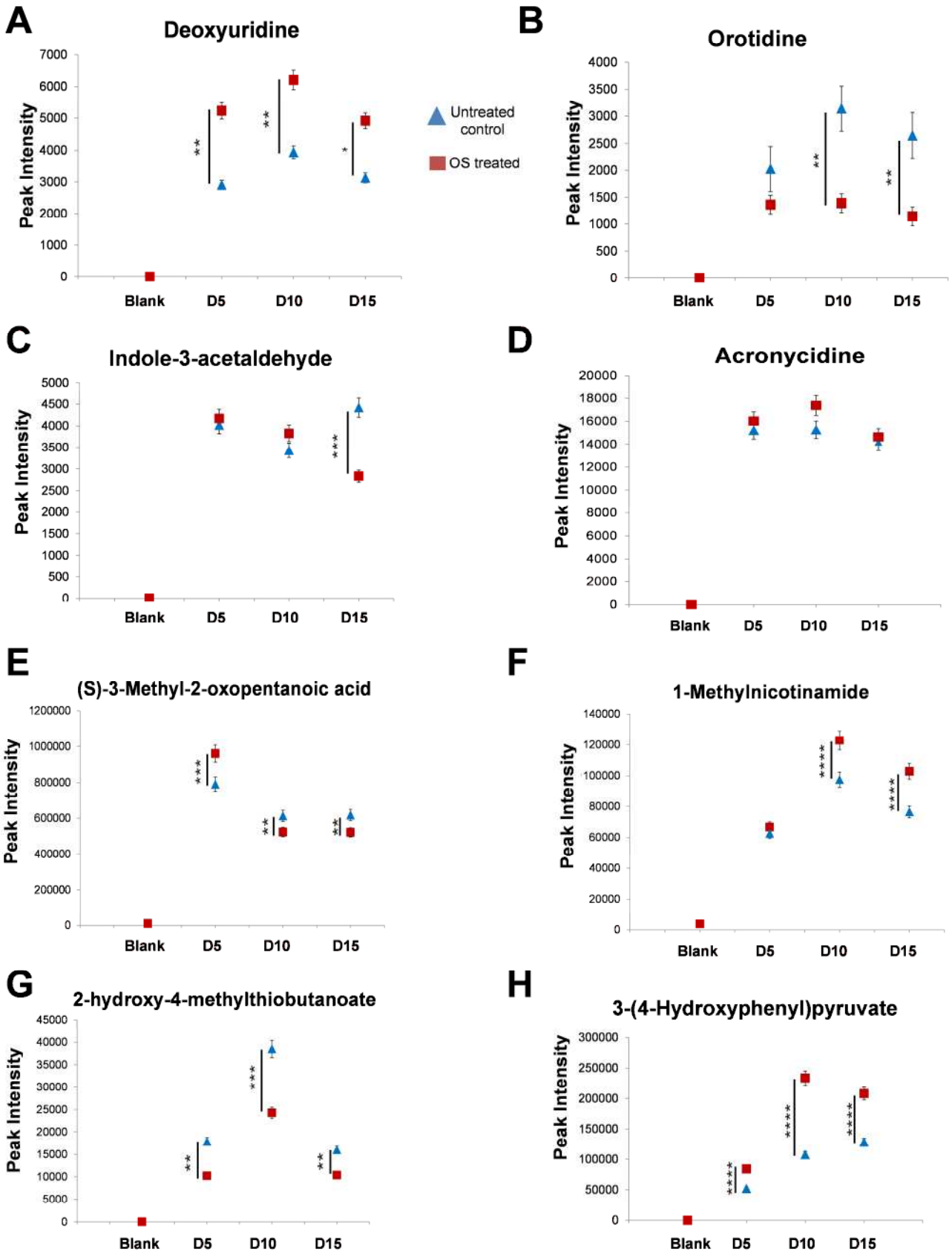
A
Deoxyuridine
Peak Intensity
Blank
D5
D10
D15
Untreated control
OS treated
B
Orotidine
C
Indole-3-acetaldehyde
D
Acronycidine
E
(S)-3-Methyl-2-oxopentanoic acid
F
1-Methylnicotinamide
G
2-hydroxy-4-methylthiobutanoate
H
3-(4-Hydroxyphenyl)pyruvate

Figure 4.

SUPPLEMENTARY FIGURES

Non-destructive characterisation of mesenchymal stem cell differentiation using LC-MS-based metabolite footprinting

Amal Surrati [1], Rob Linforth[2], Ian Fisk [2], Virginie Sottile [1]*, Dong-Hyun Kim [3]*.

[1]Wolfson Centre for Stem Cells, Tissue, Engineering and Modelling (STEM), School of Medicine, The University of Nottingham, CBS Building - University Park, Nottingham NG7 2RD (U.K.)

[2]Division of Food Sciences, University of Nottingham, Sutton Bonington Campus, Sutton Bonington, Leicestershire, LE12 5RD (U.K.)

[3]Centre for Analytical Bioscience, Division of Molecular and Cellular Sciences, School of Pharmacy, The University of Nottingham, Nottingham, NG7 2RD (U.K.)

*Correspondence to: Email: virginie.sottile@nottingham.ac.uk Tel: +44 1158231235

Email: dong-hyun.kim@nottingham.ac.uk Tel: +44 1157484697

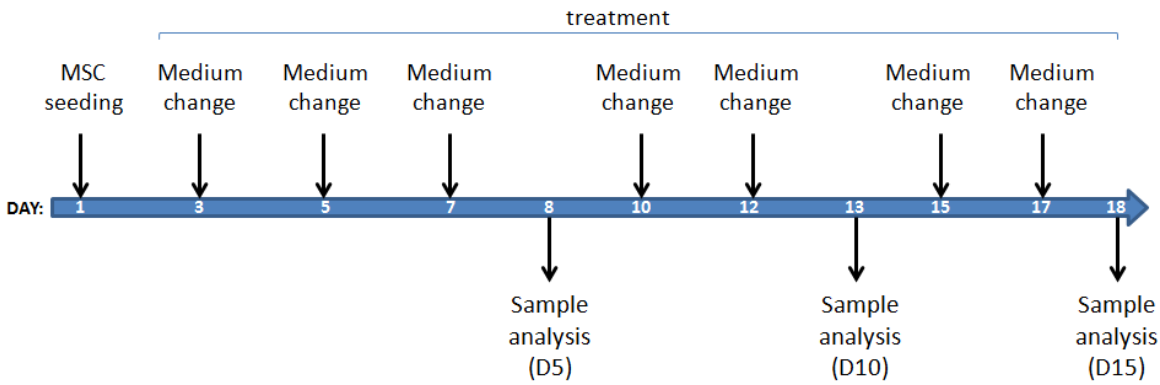

Supplementary Figure 1: Timeline of the experiment and sample collection after 5 (D5), 10 (D10) and 15 (D15) days of treatment.

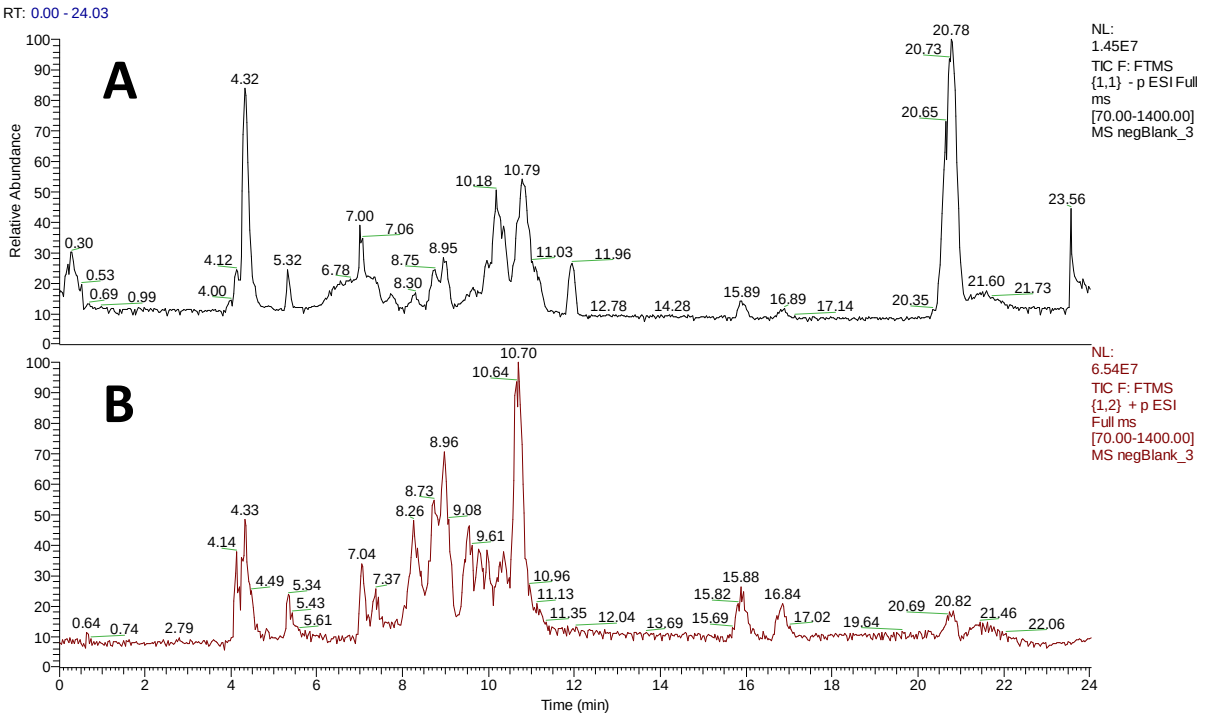

Supplementary Figure 2: Typical total ion count (TIC) chromatograms of a standard control spent medium. (A) ESI negative mode, (B) ESI positive mode

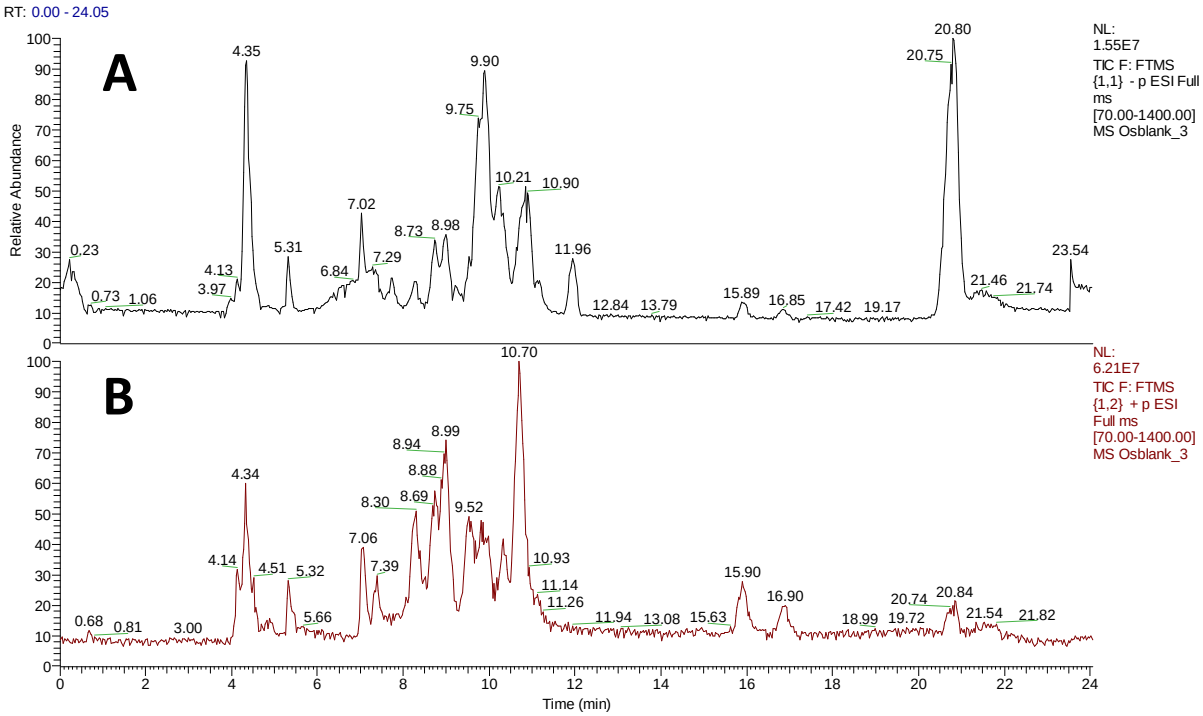

Supplementary Figure 3: Typical total ion count (TIC) chromatograms of an OS-treatment spent medium. (A) ESI negative mode, (B) ESI positive mode.

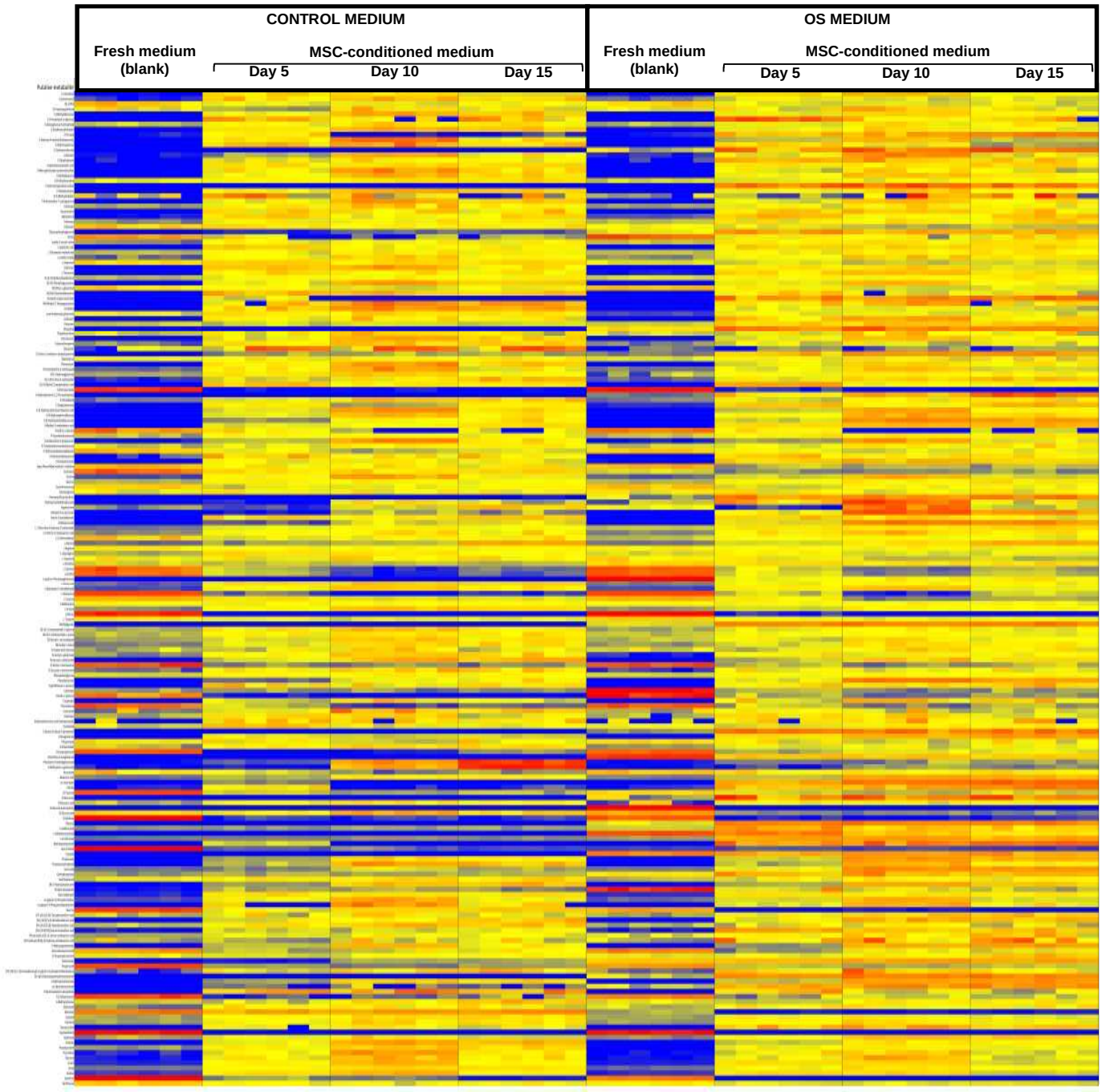

Supplementary Figure 4: Heatmap showing fold changes based on individual intensities of 195 metabolites which were increased in MSC-conditioned medium compared to fresh medium (blank) (n=6). Colours of blue (low) to yellow and red (high) represent increasing levels of metabolites.